Applied-Field MPD Thruster with Magnetic-Contoured Anodes

IEPC-2015-169／ISTS-2015-b-169

Presented at Joint Conference of 30th International Symposium on Space Technology and Science
34th International Electric Propulsion Conference and 6th Nano-satellite Symposium,
Hyogo-Kobe, Japan
July 4 – 10, 2015

Tatsuya Kimura[1]
Mitsubishi Heavy Industries, Ltd, Nagoya, Aichi, 455-8515, Japan

Kohei Kojima[2], Masaaki Yasui[3]
Mitsubishi Heavy Industries, Ltd, Komaki, Aichi, 485-8561, Japan

Daisuke Ichihara[4],Tomoki Uno[5], Hisashi Kataoka[6], Akira Iwakawa[7], Akihiro Sasoh[8]
Nagoya University, Nagoya, Aichi, 464-8603, Japan

Shigeru Yokota [9]
University of Tsukuba, Tsukuba, Ibaraki, 305-8573, Japan

Abstract: The performance of two types of steady state Applied-Field (AF) magneto-plasma-dynamic thrusters (MPDT) with a hollow cathode and a magnetic-contoured anode has been investigated. Thrust and discharge voltage on the MPDT were measured varying propellant mass flow rate, discharge current, applied magnetic field strength and cathode position. Analyzing the result, the characteristics for higher thrust efficiency were obtained as below. The axial distance between cathode and anode should be shorter so that the discharge current field is effective for hall acceleration and swirl acceleration. Supplying part of the propellant in the outer cathode increased the thrust. Less divergence of magnetic field increased the thrust because the magnetic field in axial direction generated hall acceleration and swirl acceleration. As a measured result, the maximum thrust reached 48mN. The thrust efficiency was 8% at 1250 sec of specific impulse.

Nomenclature

AF = Applied-Field
B = applied magnetic field
D = cathode-anode distance
F = thrust
HC = hollow cathode
I_{sp} = Specific impulse
J_d = discharge current
MPD = Magneto-Plasma-Dynamic

[1] Senior Assistant Manager, Space Systems Department, tatsuya_kimura@mhi.co.jp.
[2] Engineering Manager, Department Name, and kohei_kojima@mhi.co.jp.
[3] Manager, Department Name, and masaaki_yasui@mhi.co.jp.
[7] Assistant Professor, Department of Aerospace Engineering iwakawa@nuae.nagoya-u.ac.jp.
[8] Professor, Department of Aerospace Engineering, sasoh@nuae.nagoya-u.ac.jp.
[9] Associate Professor, Department of Engineering Mechanics and Energy, yokota@kz.tsukuba.ac.jp.

MPDT = Magneto-Plasma-Dynamic Thruster
$\dot{m}$ = propellant mass flow
$\dot{m}_{hc}$ = propellant mass flow rate in the hollow cathode
$\dot{m}_{ok}$ = propellant mass flow rate in the outer hollow cathode
P = input power
SF = Self-Field
V_d = Discharge voltage
η = Thrust effiency

I. Introduction

The electric propulsion (EP) thruster is capturing attention in the satellite market and the exploration program[1). It has higher specific impulse (Isp) compared to the chemical propulsion thruster, which enables satellite users to reduce launch cost and increase the weight of mission components. Thus, high thrust EP thruster could be a substitute for the chemical propulsion thruster.

A steady state magneto-plasma-dynamic thruster (MPDT) is one of the most promising electric propulsion (EP) thrusters which generate high thrust (Fig. 1). MPDT has several advantages: higher thrust density, variable Isp, a structural simplicity and higher flexibility in propellant types. However MPDT has rarely been equipped with a satellite due to two reasons. One reason is the short lifetime caused mainly by the sharp-edged cathode erosion for the local discharge current. The other reason is the lower thrust efficiency than that of other EP thruster, such as ion engines or Hall thrusters. Instead of the sharp-edged cathode, a hollow cathode is considered to be more effective in the sense that it improves the cathode's lifetime.

A 100A-class hollow cathode for high thrust MPDT is under development by our group. The performance of two types of Applied-Field MPDTs equipped with our hollow cathode and magnetic-contoured anodes has been investigated. Thrust and discharge voltage on the MPDT were measured varying propellant mass flow rate, discharge current, applied magnetic field strength and cathode position. In this paper, 100A-class hollow cathode operation results and Applied-Field MPDT performance are reported.

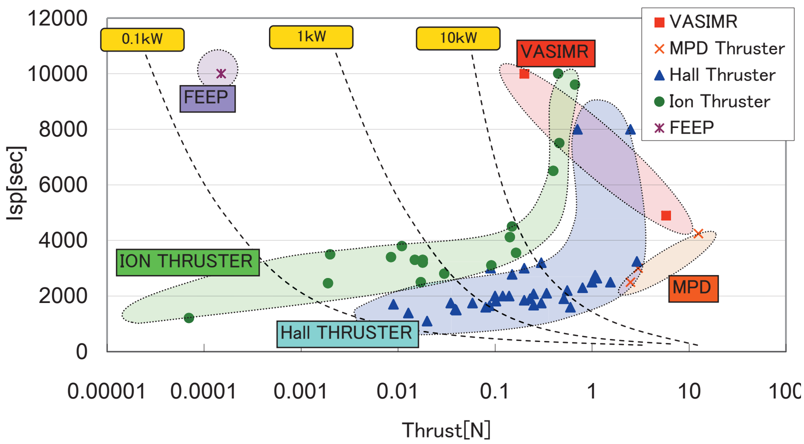

Figure 1. Thrust vs Isp in major EP systems

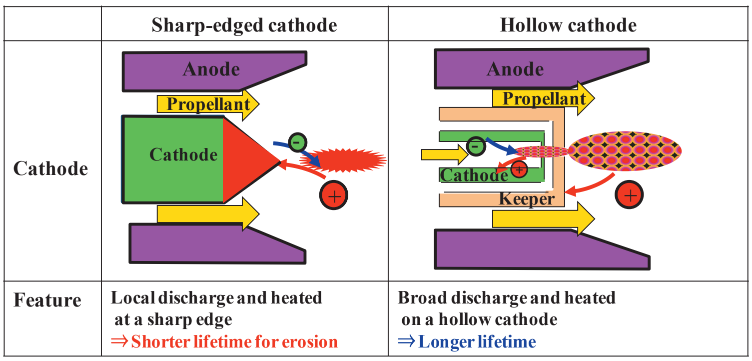

Figure 2. Sharpe-edged Thrust vs Isp in major EP systems

II. 100A-class hollow cathode development status

The 100A-class hollow cathode in our group is shown in Figure. 3. It consists mainly of an insert, a cathode body wrapped in a heater, and a keeper electrode. The insert is the thermionic electron emitter. It is made of Lanthanum hexaboride (LaB6) for higher emission current density and less sensitivity to impurities [2, 3]. The length and diameter of the inset are determined by plasma density distribution in the axil and emission current density and discharge current. The cathode body structure and size are designed by thermal analysis. The heater raises the insert temperature to emissive temperature to start the discharge. High voltage between the keeper and the insert is applied to start the discharge in a hollow cathode.

The hollow cathode was experimented to demonstrate the high current emission capability. As a result, the hollow cathode successfully operated at up to 100 A of discharge current for 120seconds with xenon propellant (Fig. 2).

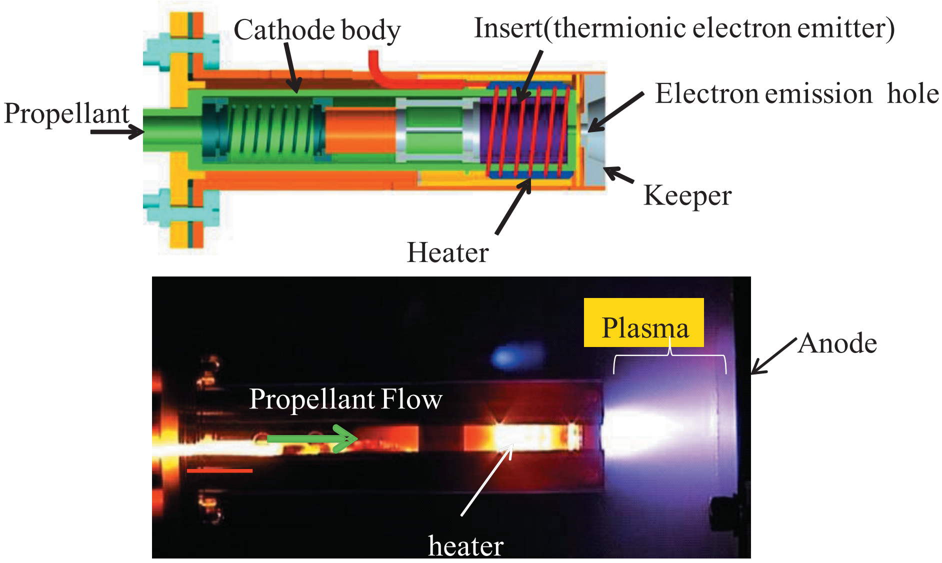

Figure 3. Schematic of the hollow cathode and a photograph of cathode discharge

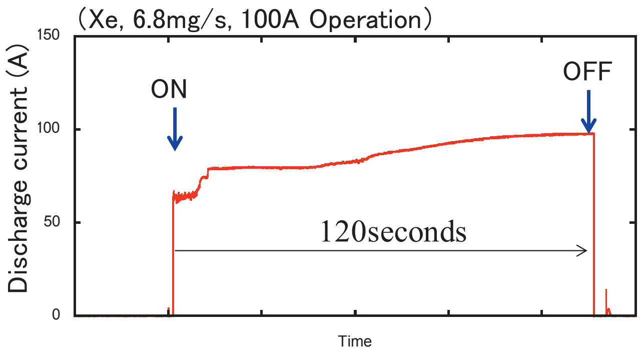

Figure 4. The hollow cathode operation anode current data

III. Design of steady state Applied-Field (AF) MPDTs

A. Generation of a magnetic field

There are two methods for generating magnetic fields, Self-Field (SF) and Applied-Field (AF). A high-current electric arc is driven between the anode and cathode to ionize a propellant gas in order to create plasma. A magnetic field is generated by the electric current returning to the power supply through the cathode. This self-induced magnetic field interacts with the electric current flowing from the anode to the cathode to produce the electromagnetic Lorentz force that pushes the plasma out of the engine, generating thrust. MPDTs are usually classified either in the Self-Field (SF) type, which is fully based on the pure self-field mechanism, or in the – generally lower-power – Applied-Field (AF) type, where an external coil is equipped to provide additional magnetic field to help stabilize and accelerate the plasma.

Since the SF magnetic field is proportional to the square of the current, a larger current such as several kA class is required for generating efficient thrust. Thus, it is difficult for SF MPDT to operate under a steady state. Furthermore, there is a case in which electrode erosion is caused by the local discharge current even in a quasi-stationary state operation. Several hundred kW or more power is required for SF MPDT.

Meanwhile, the discharge current and the magnetic field strength can be controlled independently in AF MPDT, and the risk of the electrode erosion is reduced to a relatively low current such as several hundred A. By increasing the magnetic field strength to a power of several tens kW, it can achieve high thrust efficiency. In this study, AF type is adopted for the magnetic field generation method.

B. Acceleration principle of the AF MPDT

Hall acceleration and swirl acceleration are the major acceleration component of the AF MPDT.

Hall acceleration $J_\theta \times B_r$ ($J_\theta \propto J_r \times B_z$)

The interaction between the azimuthal (Hall) discharge current J_θ and the radial magnetic field B_r yields an axial Lorentz force. J_θ is generated by the interaction between the radial discharge current J_r and the axial magnetic field B_z.

Swirl acceleration $J_r \times B_z$

The interaction between the radial discharge current J_r and the axial magnetic field B_z yields an azimuthal Lorentz force that causes the plasma to rotate. The energy recovered from this swirl motion can partially give rise to an axial thrust component by the anode nozzle or the magnetic nozzle.

The other accelerations are as below

>The interaction between the radial discharge current J_r and the self-induced azimuthal magnetic field B_θ results in a thrust component similar to that of the SF MPDT.

>A gasdynamic component similar to that of Arcjets.

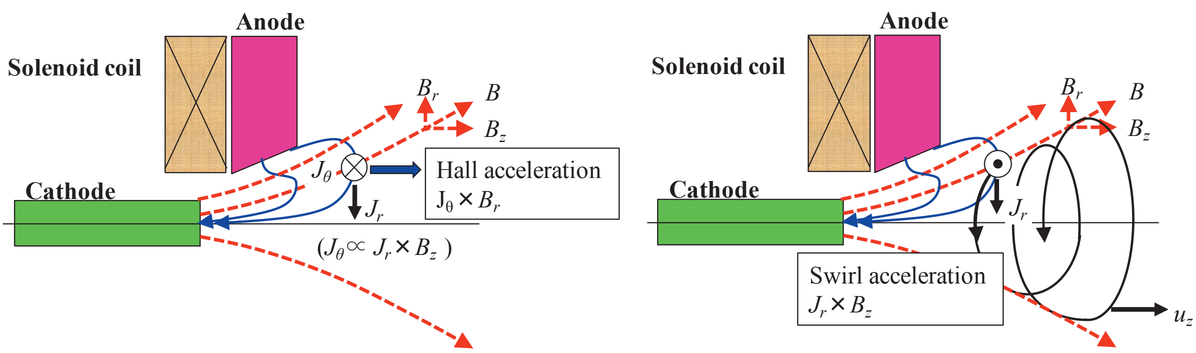

Figure 5. Schematic of Hall acceleration principle and Swirl acceleration principle

C. Design subjects and study directions

The thrust provided by SF MPDT is formulated by use of the following equation. Various studies have been conducted for optimizations of anode shape by the analysis and the examinations.

$$F=(\mu J^2)/4\pi\,[3/4+\ln(r\_a/r\_c)]$$

Here, μ , r_a and r_c mean vacuum magnetic permeability, radius of anode and radius of cathode respectively.

Meanwhile, an optimization guideline for the magnetic field and the anode contour is not established because the AF MPDT brings out complex interactions of the discharge current with magnetic field in various directions. In this study, in order to come out with the design directions for the higher thrust efficiency of AF MPDT, two types of solenoid coils with different magnetic fields were manufactured and the performances were investigated for each. The manufactured anodes contour lies along the magnetic field lines to effectively utilize the generated magnetic field. The developing 100A class hollow cathode is also used as a cathode. The two types of generated magnetic fields and the anode nozzle contours are shown in Figure 6. One model has the magnetic field lines which are about

45 degrees on the anode wall(call "$Br \fallingdotseq Bz$"), the other model has the magnetic field lines which are about less than 45 degrees on the anode wall(call "$Br < Bz$").

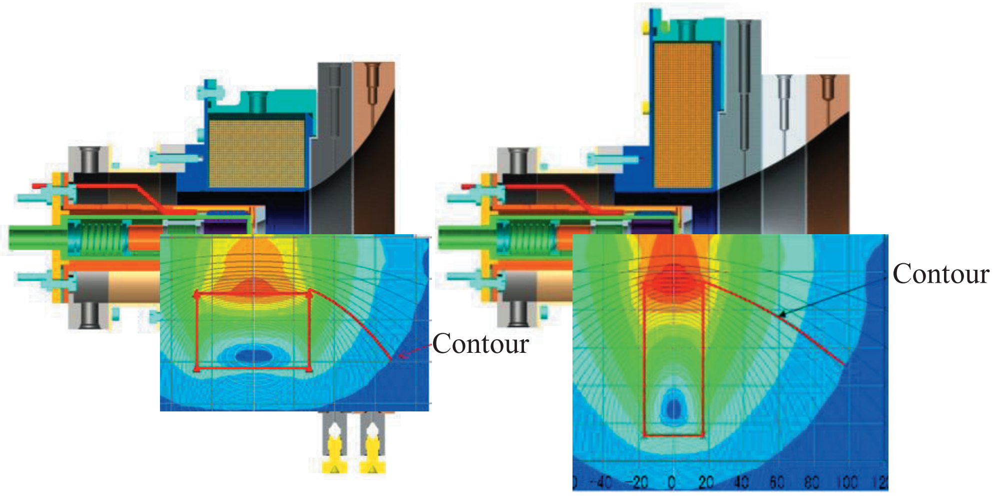

(a) "$Br \fallingdotseq Bz$" (b) "$Br < Bz$"

Figure 6. Magnetic field contour by solenoid coil and anode nozzle contour

IV. Experimental Setup

The experiments in this study were conducted in a vacuum chamber whose diameter and length are 2m and 4m respectively at Nagoya University. The vacuum chamber was evacuated using a turbo molecular pump (3200L/s) backed by a rotary pump (33.3L/s). The ambient pressure in the vacuum chamber was measured by an ionization vacuum gauge and a pirani gauge. The ambient pressure without propellant flow was 10^{-3} Pa; at the mass flow rate of 1.25 mg/s, ambient pressure was 5.5×10^{-2} Pa. Thrust was measured using a pendulum type thrust stand. It consists of a stand arm, a vacuum bellows and two radial bearings. A differential transformer was used to detect the pendulum oscillation amplitude. Thrust was measured three times and calculated the mean and standard deviation in each operating condition. Thruster operating time was about 7 seconds.

The operation conditions and measured values are tabulated in Table 1. Thrust, discharge voltage and keeper voltage were measured varying propellant mass flow rate, discharge current, magnetic field and distances between cathode and anode. Evaluation parameters are thrusts and specific impulse (Isp), thrust efficiency(η), thrust power ratio.

- $Isp=F/\dot{m}$
- Thrust efficiency $\eta=F^2/(2\dot{m}P)$
- Thrust power ratio $=F/P$

Here, $\dot{m}$ and P mean propellant mass flow rates and input power respectively.

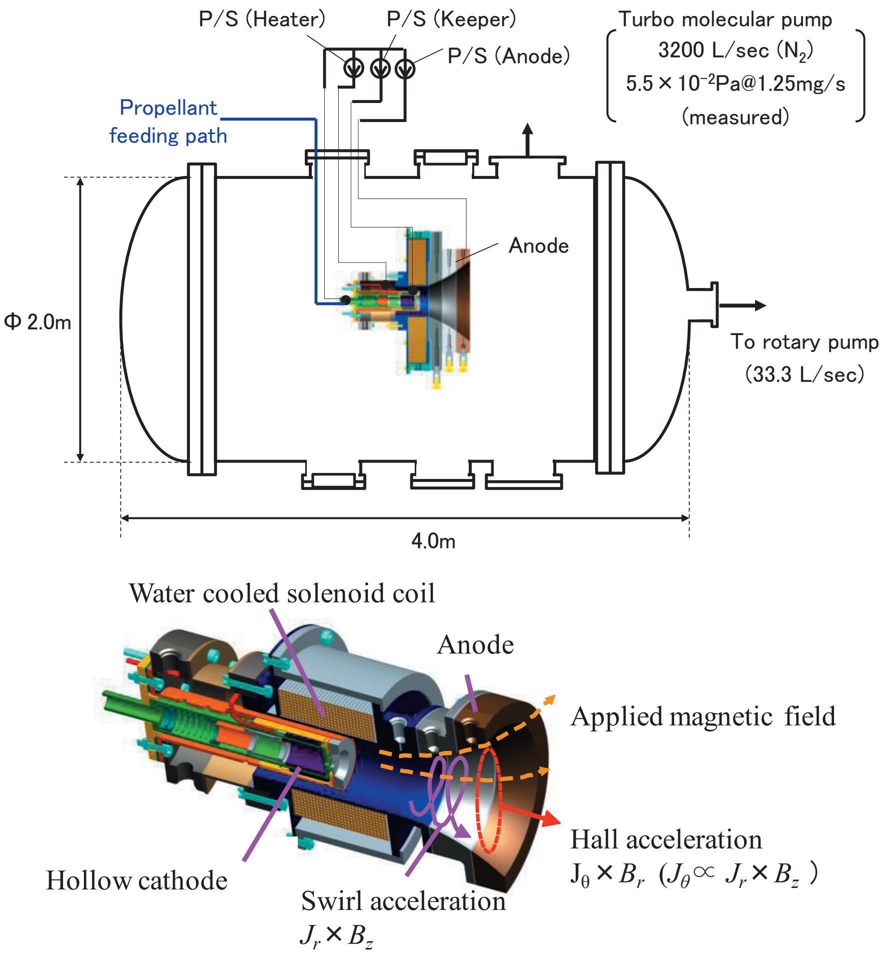

Fig 7. Schematic of experimental setup and MPDT head

Table 1. Operation conditions

Controlled parameter		
Propellant		Xe, H_2
Mass flow rate (mg/s)	$\dot{m}$	0.9～10.3
Discharge current (A)	J_d	10、20、30
Keeper current (A)	J_k	2
Solenoid coil current (A)	J_c	1（25mT） ～10（250mT）
Distance between cathode and anode (mm)	D	26.0、30.8
Propellant mass flow rate outer the hollow cathode / Total propellant mass flow rate	$\dot{m}_{bk}$ / $\dot{m}$	0%、20%、50%、80%
Measured parameter		
Thrust (mN)	F	
Discharged voltage (V)	V_d	
Keeper voltage (V)	V_k	
Coil voltage (V)	V_c	

V. Results and discussions

A. Dependency on J_d, B, and $\dot{m}$

F and V_d increase linearly with an increase in either J_d or B (Fig. 8). The exhaust plume shows that the discharge current distributes more downstream as exhaust velocity increases by higher J_r or higher B (Fig. 9). The plume rotation was observed as being higher in B. It is assumed that the plume rotation is generated by an increase in the plasma angular momentum by the swirl acceleration.

η was higher as $\dot{m}$ decreased at the same J_d (Fig. 10). It is considered that Lorentz force does not depend on $\dot{m}$ and the exhaust velocity increased at lower $\dot{m}$. However, plasma discharge was unstable when $\dot{m}$ was too low. In the future works, optimization of $\dot{m}$ to archive both higher η and discharge stability is needed.

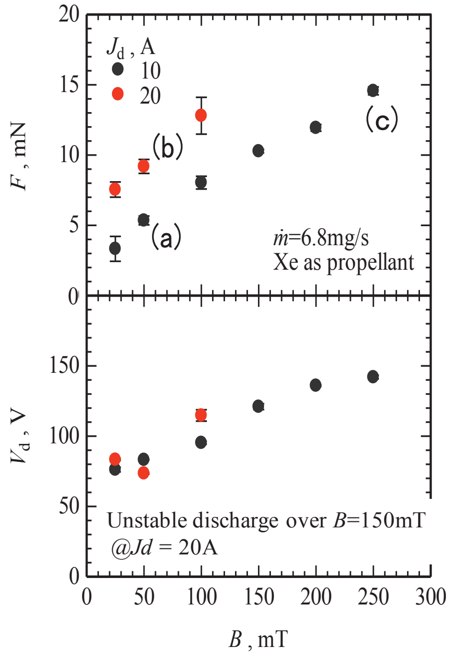

Figure 8. F and V as a function of B

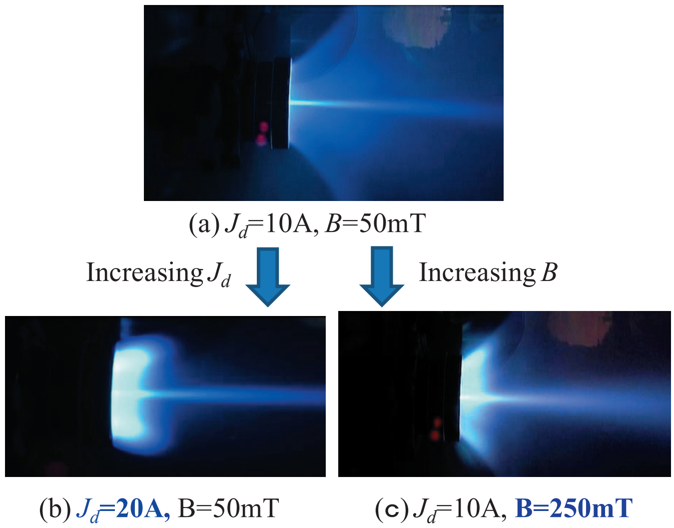

Figure 9. Exhaust plume varying J_d and B

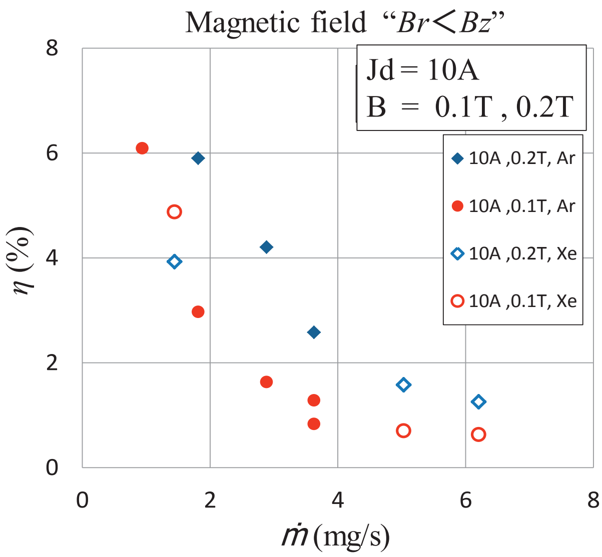

Figure 10. η as a function of $\dot{m}$

B. Dependency on distance between cathode and anode (*D*)

In order to investigate the effect of *D* on the thrust performance, examinations were conducted varying the position of the cathode (Fig. 11). *F* and V_d increased with decrement of *D*. At the same J_d (=10A), the component of J_z was smaller and that of J_r was larger with decrement of *D*. The larger J_r can generate larger hall acceleration and swirl acceleration.

On the other hand, placing the cathode upstream can promote propellant to diverge and distribute uniformly in the anode. There is examination result that stable operation $\dot{m}$ range in *Jd* and *B* expanded placing cathode upstream 4). In the future works, optimization of *D* is needed for higher η.

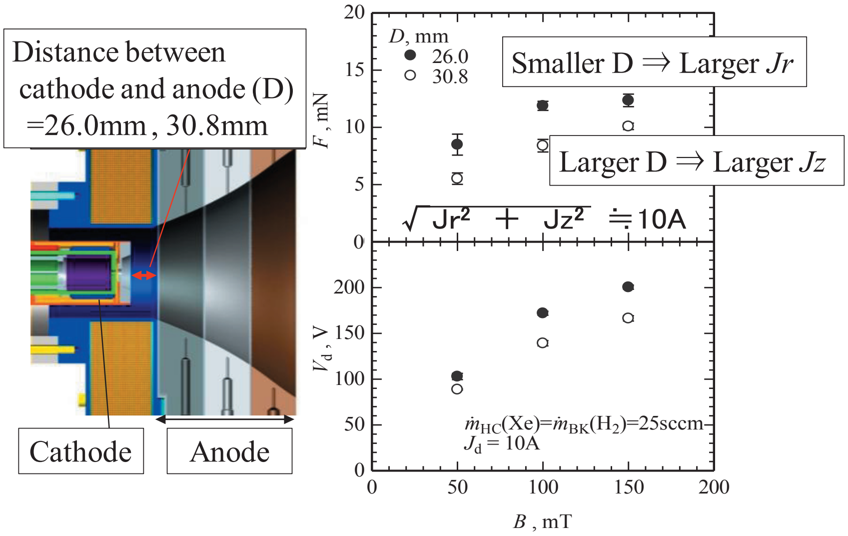

Figure 11. The effect of D on the thrust performance

C. Dependency on distribution of propellant flow in MPDT head

Supplying part of propellant to the outer hollow cathode raised *F* up to 1.4 times as compared to full supplying propellant to the hollow cathode (Fig. 12). It is considered that the propellant distributed uniformly in the anode and the Lorentz force worked effectively. Furthermore supplying propellant with lower molecular weight is expected to raise *F* due to higher exhaust plasma velocity. In this study, hydrogen was supplied to the outer hollow cathode. As a result F increased up to 1.8 times as compared to supplying the same amount of Xe gas (Fig. 13).

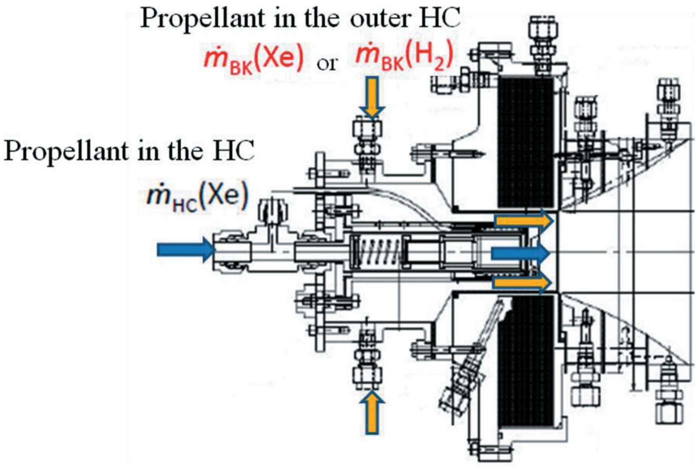

Figure 12. Schematic of Supplying part of propellant in the outer hollow cathode

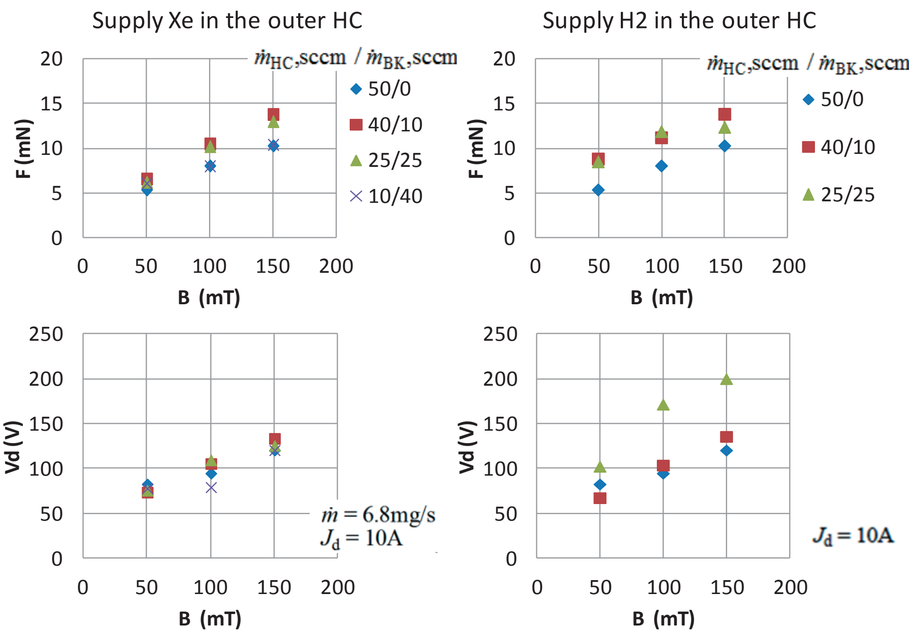

Figure 13. *F* and *V* as a function of *B* supplying part of propellant in the HC

D. Dependency on Magnetic field and anode contour

As mentioned above, in order to investigate the effect of magnetic contour and anode contour on the thrust performance, two types of AF MPDT were manufactured and examined. Thrust efficiency (*η)* as a function of *Isp* with two models ("*Br*≒*Bz*","*Br*<*Bz*") are shown in Figure. 14. A tendency that *η Isp* ratio (*η/Isp)* which is proportional to thrust power ratio (*F*/*P*) of "*Br*<*Bz*" is higher than that of "*Br*≒*Bz*" is shown. When the magnetic field lines are about 45 degrees ("*Br* ≒ *Bz*"), hall acceleration is optimum. The above mentioned result("*Br*<*Bz*" is better than "*Br*≒*Bz*") indicates that less divergence of magnetic field ("*Br*<*Bz*") increases thrust because magnetic field in axial direction generates hall acceleration and swirl acceleration.

<u>Hall acceleration</u> $J_\theta \times B_r$ ($J_\theta \propto J_r \times B_z$) *Br* ≒ *Bz*" is optimum

<u>Swirl acceleration</u> $J_r \times B_z$

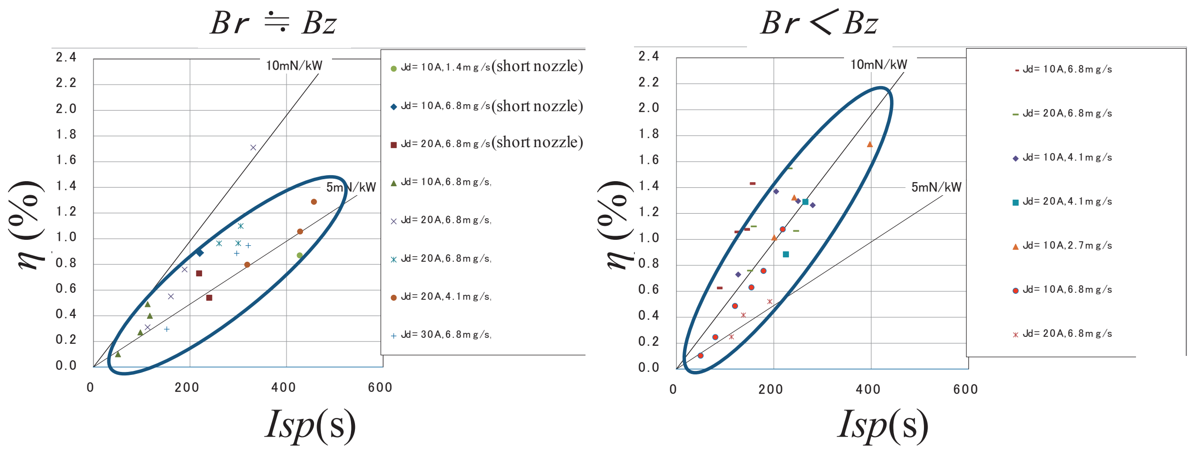

Figure 14. Thrust efficiency (*η)* as a function of *Isp* compared with two model ("*Br*≒*Bz*","*Br*<<u>*Bz*</u>")

E. Maximum performance

Thrust efficiency (η) as a function of *Isp* with the "*Br*<*Bz*" model is shown in figure. 15. The thrust efficiency was 8% at 1250 sec of specific impulse. The maximum *F* was recorded 47mN.

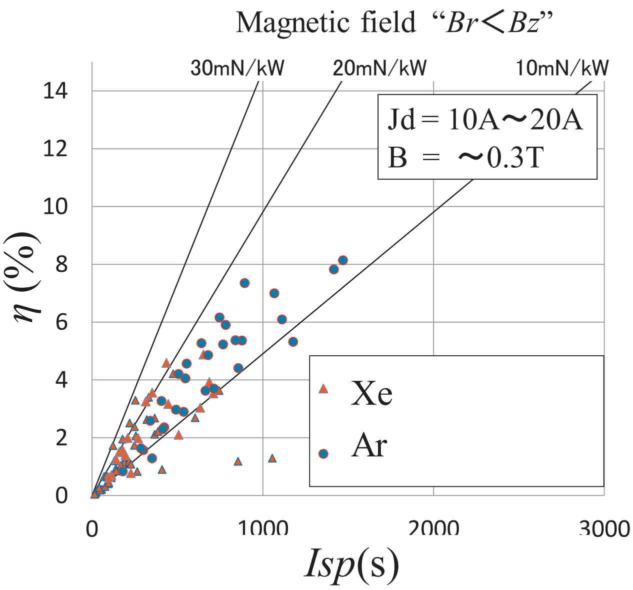

Figure 15. Thrust efficiency (η) as a function of *Isp* with the model ("*Br*<*Bz*")

VI. Conclusions

Our hollow cathode under development was demonstrated in continuous operation of about 120 seconds at 80-100A.

The performances of prototype AF MPDT were obtained. Obtained characteristics are as below.

- *F* increases when the distance between cathode and anode (*D*) is small. When *D* was small, the component of J_z was smaller and that of J_r was larger at the same J_d. The higher J_r can generate larger hall acceleration and swirl acceleration.
- Supplying part of the propellant to the outer hollow cathode raised *F* up to 1.4 times as compared to full supplying propellant in the hollow cathode.
- Less divergence of magnetic field ("*Br*<*Bz*") increases thrust because magnetic field in axial direction generates hall acceleration and swirl acceleration.

VII. References

[1]http://www.globalspaceexploration.org/wordpress/

[2]D. Goebel, I. Katz, "Fundamental of Electric Propulsion," Wiley, pp.243-324, 2008.

[3]D. Goebel, E. Chu, "High Current Lanthanum Hexaboride Hollow Cathodes for High Power Hall Thrusters," IEPC Paper 2011-053, 2011.

[4]G. Krulle, A. Sasoh, "Technology and Application Aspects of Applied Field Magnetoplasmadynamic Propulsion," Journal of Propulsion and Power, Vol. 14, No. 5, 1998, pp754-763